

Figure S1. Kv1.3 expression increases during degeneration in *C3H3/HeOuJ rd1* mouse model. Kv1.3 channel RNA levels in OBCs from *C57BL/6J* mice (p 210) and *C3H3/HeOuJ rd1* mice (p105) (p210), **p=0.015.

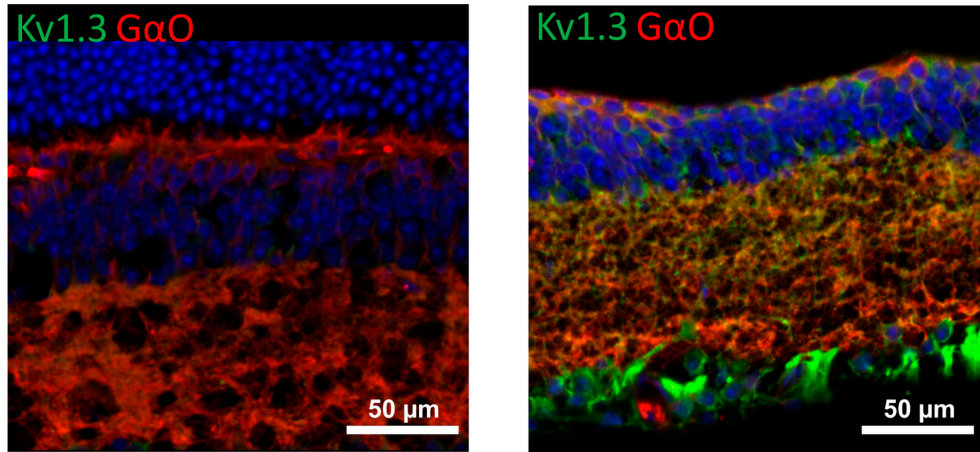


Figure S2. Kv1.3 expression increases during degeneration in OBCs. Anti-Kv1.3 immunolabeling (green) on retinal cryosection of *C57BL/6J* mice at p210 (left), *FVB rd1* mice at p210 (right). OBCs were identified by anti-GαO immunolabeling (red). Images were taken as single optical sections (770 nm) on a Zeiss LSM880 confocal microscope (40×, NA: 1.3).

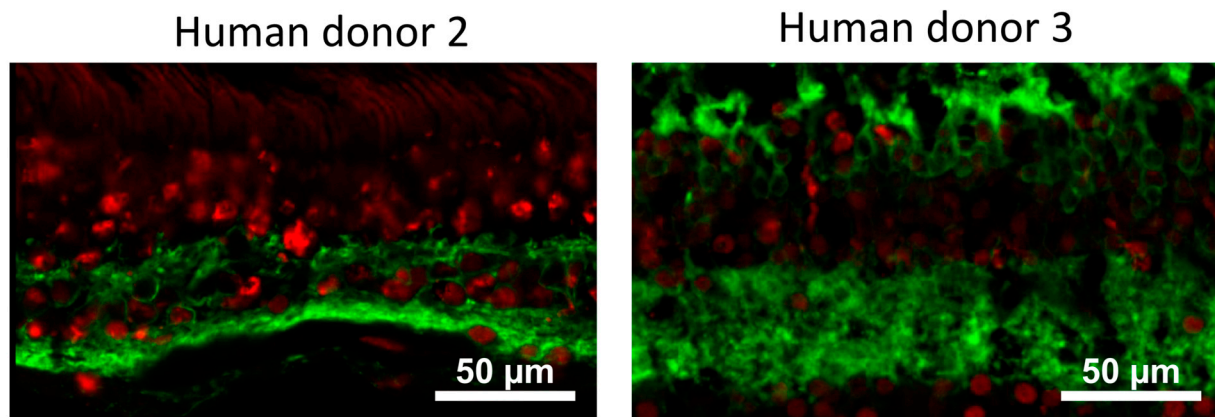


Figure S3. TUNEL+ (red) OBCs (green) in the human retina at 0 days of culture from 2 different donors (donor 2 left, donor 3 right). OBCs were stained with anti-G α O immunolabeling. Images were taken as single optical sections (770 nm) on a Zeiss LSM880 confocal microscope (40 \times , NA: 1.3).

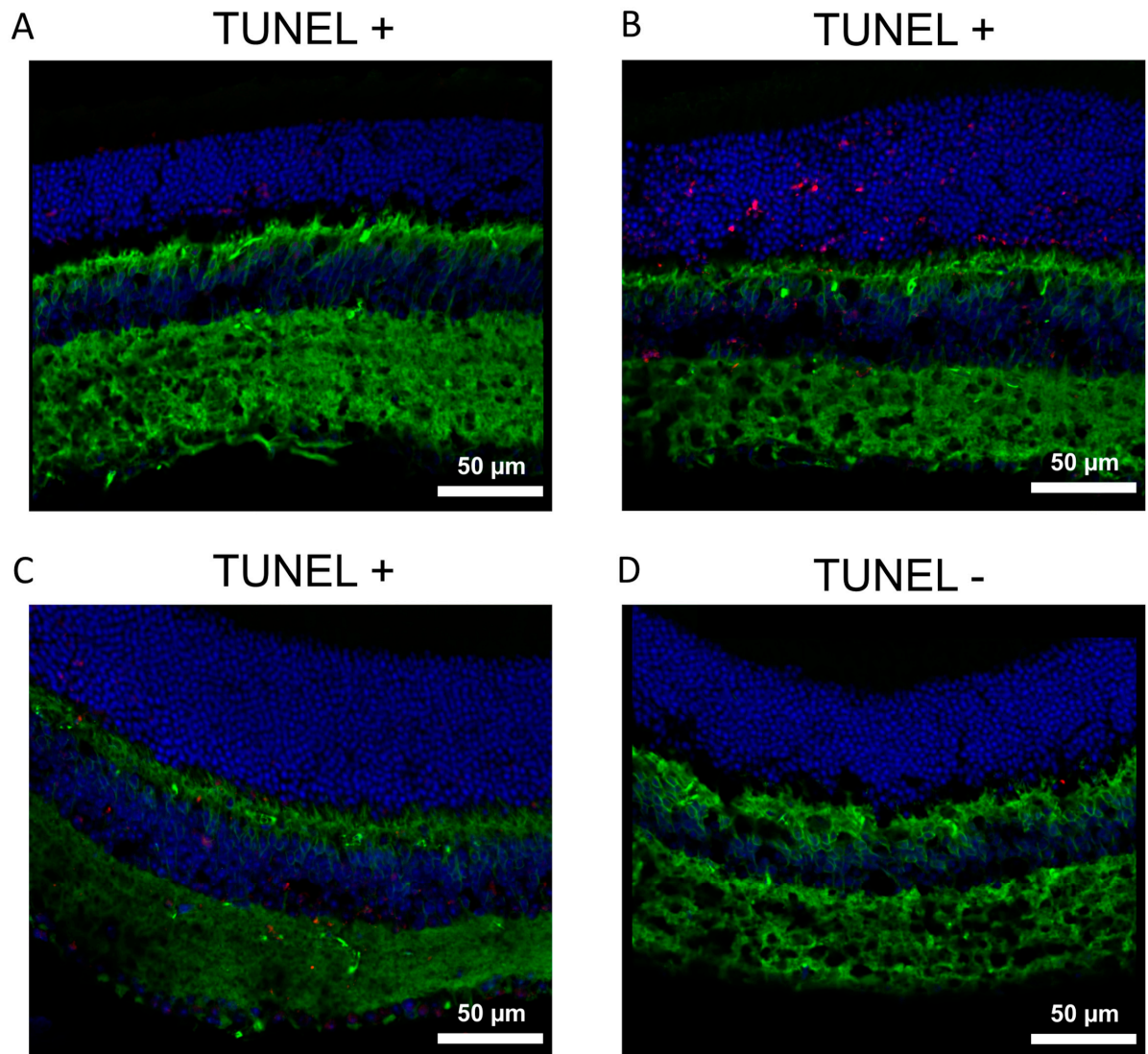


Figure S4. (A)(B)(C) TUNEL+ (red) OBCs (green) in *C57BL/6J* retina slice from 3 biological samples; (D) TUNEL - staining as a negative control on *C57BL/6J* retina slice. OBCs were stained with anti-GαO immunolabeling. Images were taken as single optical sections (770 nm) on a Zeiss LSM880 confocal microscope (40×, NA: 1.3).

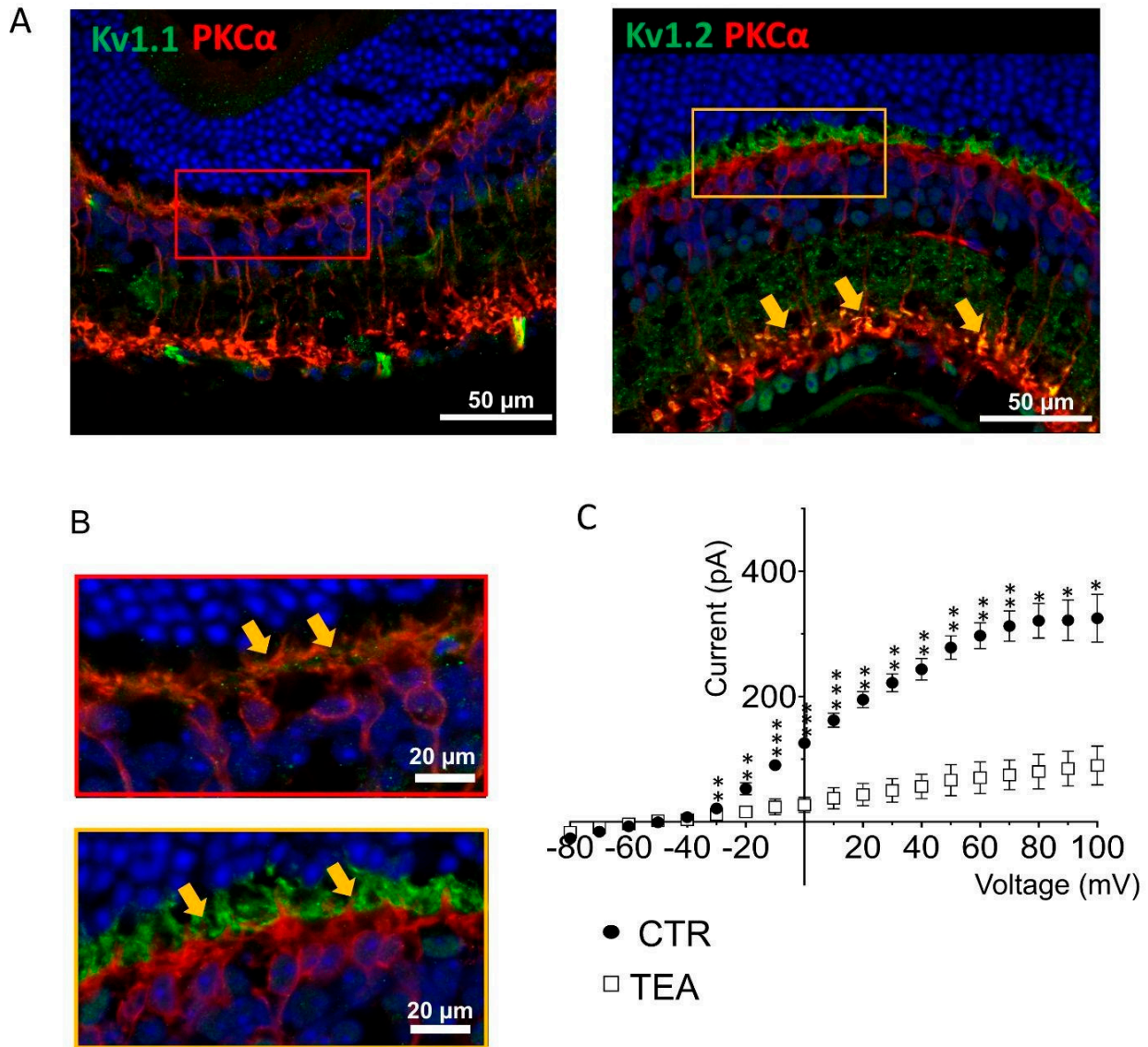


Figure S5 Kv1.1 and Kv1.2 are localized in the OBCs dendrites and axon terminals in the healthy mouse retina. (A) anti-Kv1.1 immunolabeling (green) (left) and anti-Kv1.2 (right) on retinal cryosection of *C57BL/6* mice at p210. OBCs were identified by anti-PKC α immunolabeling (red). Images were taken as single optical sections (770 nm) on a Zeiss LSM880 confocal microscope (40 \times , NA: 1.3); (B) Magnification of figure A with Kv1.1 (top) and Kv1.2 (bottom); Kv1.1 is expressed in OBC dendrites and Kv1.2 in OBC dendrites and axon terminals. (C) I/V relationship (step protocol from -80 mV to 100 mV, Δ = 10 mV) in control condition (CTR, n= 3) and with the bath application of the potassium channel blocker 10 mM TEA (n=3) (-30 mV, **p=0.0144; -20 mV, **p=0.0037; -10 mV ***p=0.00033; 0mV ***p=0.00075; 10mV ***p=0.0030; 20mV, **p=0.0037; 30mV, **p=0.0066; 40mV, **p=0.0094; 50mV, **p=0.0091; 60mV, **p=0.0089; 70mV, **p=0.0135; 80mV, *p=0.0210; 90mV, *p=0.0267; 100mV, *p=0.0375);

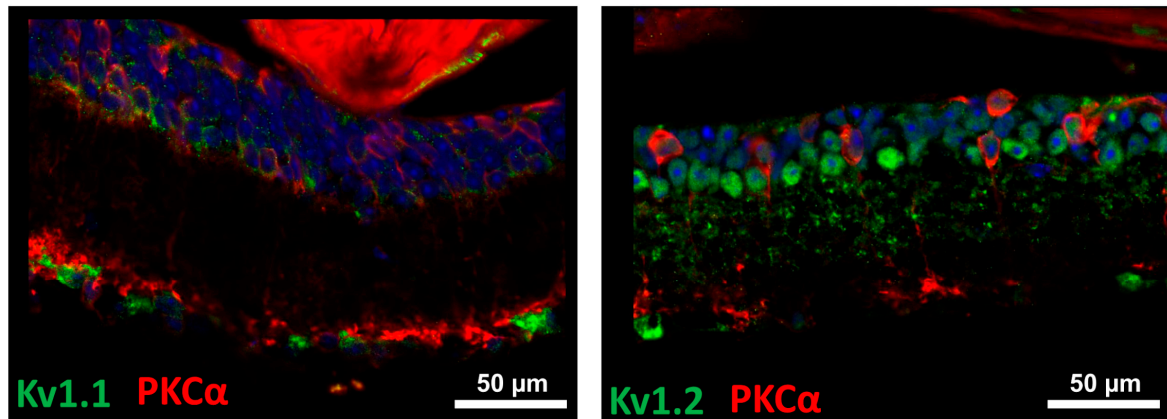


Figure S6. Kv1.1 and Kv1.2 channels expression in OBCs in *FVB rd1* retina. anti-Kv1.1 (left) and anti-Kv1.2 (right) immunolabeling (green) on retinal cryosection of *FVB rd1* mice at p210 (left). ON-RBCs were identified by anti-PKC α immunolabeling (red). Images were taken as single optical sections (770 nm) on a Zeiss LSM880 confocal microscope (40 \times , NA: 1.3).

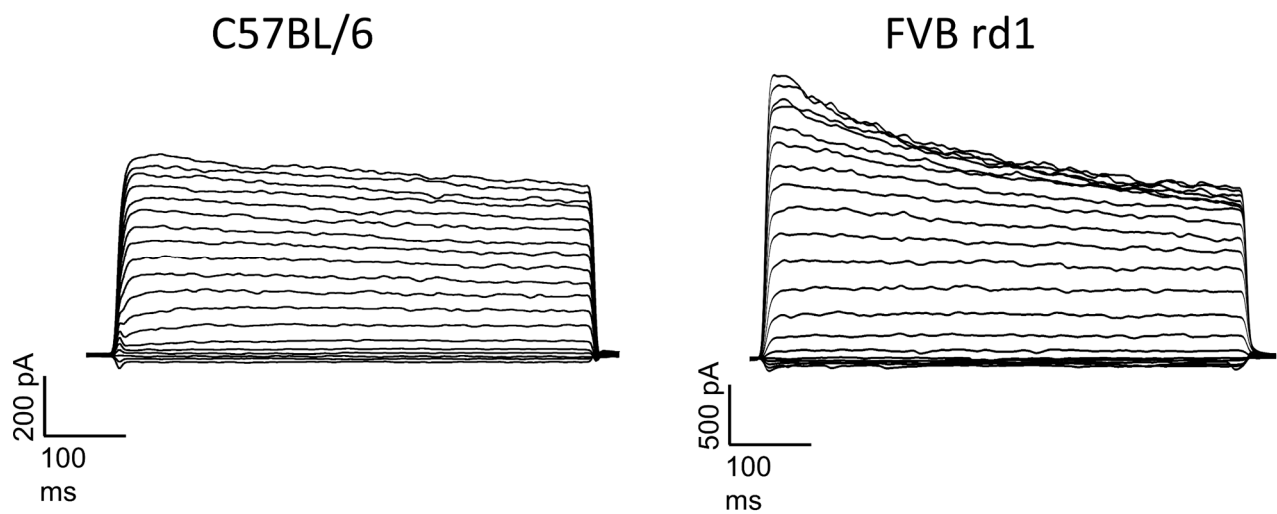
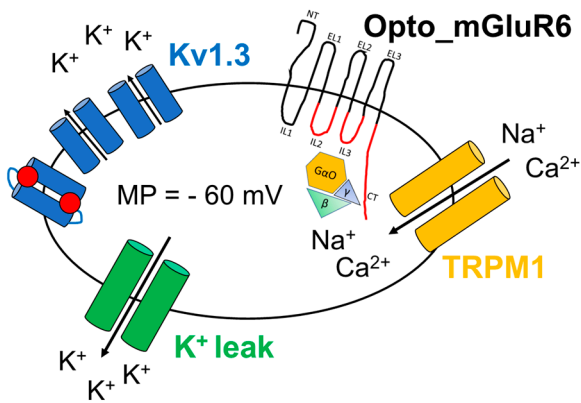
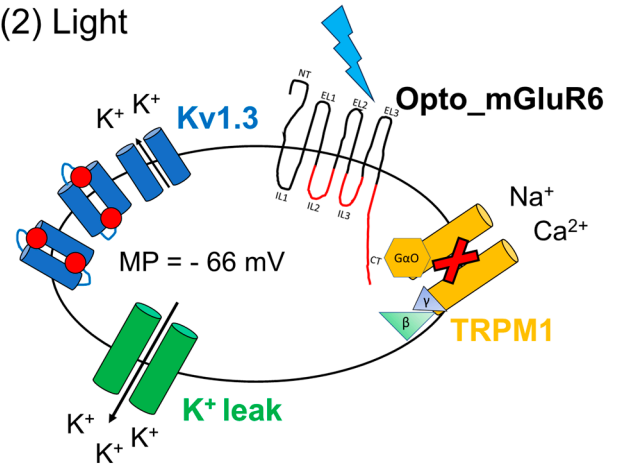


Figure S7. Example traces of voltage step protocol (-80 mV to 100 mV, $\Delta=10$ mV) for a C57BL/6J (left) and for an FVB rd1 (right) ON-bipolar cell. The off-kinetics are clearly different in the two traces, with a $\text{Tau}(\text{off})$ of 564.37 ± 147.72 ms in C57BL/6 ON-bipolar cells and a $\text{Tau}(\text{off})$ of 43.42 ± 22.43 ms in FVB rd1 ON-bipolar cells, in line with a change from expressing Kv1.1/1.2 channels in the healthy retina to expressing predominantly Kv1.3 in the degenerating rd1 retina.

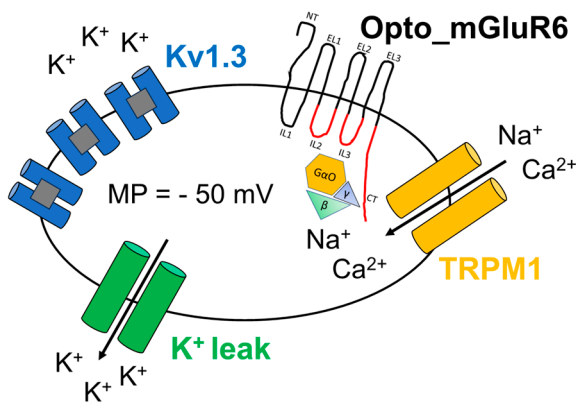
(1) Dark



(2) Light



(3) Dark + Psora-4 ■



(4) Light + Psora-4 ■

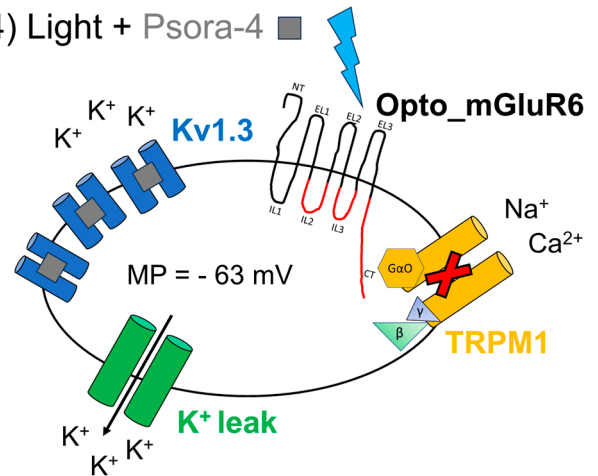


Figure S8. Cartoon depicting the potential underlying mechanism of membrane potential tuning in OBCs during optogenetic activation via Opto-mGluR6 with and without Psora-4 inhibition of Kv1.3 channels, shown in Fig. 4A. (1) In the dark, Opto-mGluR6 is inactive, TRPM1 open and depolarizing the OBC, while the majority of Kv1.3 channels is open and leak potassium channels (K⁺ leak) are hyperpolarizing. (2) Light activates Opto-mGluR6, TRPM1 closes, Kv1.3 becomes partially inactive due to hyperpolarization driven by TRPM1, leak potassium current drives membrane potential towards the potassium equilibrium potential. (3) As (1), but Psora-4 inhibits hyperpolarizing Kv1.3 channels, which depolarizes the membrane potential. (4) As (2), but now all Kv1.3 channels are blocked from the beginning by Psora-4, therefore the membrane potential may be slightly depolarized as opposed to (2). The main hyperpolarization driver is the closure of TRPM1. Note: The given membrane potentials are actual experimental average values. There may be, however, some clamping issues due to the very thin processes and high access resistances of OBCs, potentially causing a slight artificial shift in the K reversal potential.